Chapter 13

Surface Interactions of CF_2 Radicals during Deposition of Amorphous Fluorocarbon Films

Neil M. Mackie[1], Nathan E. Capps[2], Carmen I. Butoi[3], and Ellen R. Fisher[3]

[1]Mattson Technologies, 3550 West Warren Avenue, Fremont, CA 94538
[2]Advanced Energy, Inc., 1625 Sharp Point Drive, Fort Collins, CO 80525
[3]Department of Chemistry, Colorado State University, Fort Collins, CO 80523–1872

Fluorocarbon polymer film composition and CF_2 radical-surface interactions in two fluorocarbon plasmas, 100% CHF_3 and 50/50 C_2F_6/H_2, are compared. Our imaging of radicals interacting with surfaces (IRIS) technique was used to collect spatially-resolved laser-induced fluorescence (LIF) images of CF_2 radicals interacting during film growth on silicon substrates. Simulation of LIF cross-sectional data shows that 100% CHF_3 plasmas have high scattering coefficients for CF_2 radicals. These large scattering coefficients (1.65 ± 0.03) indicate CF_2 molecules are generated through plasma interactions with the substrate. In contrast, IRIS data for CF_2 from 50/50 C_2F_6/H_2 show lower scattering coefficients (0.84 ± 0.02). Films deposited during IRIS experiments were characterized using X-ray photoelectron spectroscopy (XPS) and Fourier transform infrared (FTIR) spectroscopy and were nearly identical in composition regardless of plasma system. In addition, using independent plasma reactors, fluorocarbon polymer film deposition rates were measured as a function of applied rf power for both systems and optical emission spectra (OES) were collected and compared. The role of CF_2 radicals in fluorocarbon film deposition is discussed in relation to previously proposed film formation models.

Introduction

Fluorocarbon plasmas (FCPs) have been extensively studied because of their dual ability to promote etching of a variety of substrates[1,2] and to deposit a wide range of amorphous fluorinated carbon (a-C:F) polymer films.[3,4] Polymeric fluorocarbon materials deposited from FCPs exhibit a range of advantageous properties. Namely, their good adhesion to many organic and inorganic substrates; low surface free energies and inertness; low dielectric constants (k - 1.8-2.2);[5] high biocompatibility; and structural compositions that can be changed over a broad range producing films that are specifically tailored for each application.

In Fluorinated Surfaces, Coatings, and Films; Castner, David G., et al.;
ACS Symposium Series; American Chemical Society: Washington, DC, 2001.

While an enormous body of work using fluorocarbon plasmas (FCPs) exists, details of the mechanisms for fluorocarbon polymer deposition remain unclear. Gas-phase density measurements have shown there are significant concentrations of neutral radicals and energetic ions in FCPs. These active species are important chemical precursors to etching and deposition processes.[6,7,8] One mechanism for the deposition of fluorocarbon films from FCPs comes from d'Agostino and coworkers who propose an activated growth model (AGM).[5] AGM implies that film growth occurs through interaction of CF_x radicals with an "activated" surface. This activation occurs from charged particle bombardment creating reactive sites on the surface. This mechanism was postulated after d'Agostino and coworkers observed that fluorocarbon deposition rates were proportional to CF_2 radical and electron density in FCPs.[9] It has also been determined that the deposition of fluorocarbon films from FCPs displays a non-Arrhenius behavior and that there is a negative apparent activation energy for the deposition process.[10] This suggests adsorption-desorption processes are important in film growth.

In addition to the AGM, another factor that governs the etching and deposition capacity of FCPs is the ratio of CF_x radicals to F atoms. There are a number of operating conditions that modulate this ratio: fluorocarbon starting materials with high F/C ratios produce less CF_x radicals than F atoms;[11] and the addition of hydrogen to the fluorocarbon feed drives polymerization reactions forward by directly reacting with F to form stable HF and to prevent CF_x recombination reactions.[5] Surface interactions of H atoms in FCPs are not completely understood, although surface abstraction of F by H is thermodynamically possible.[12] Thus, the surface interactions of CF_x radicals as well as the role of fluorine and hydrogen during fluorocarbon polymer film deposition are critical for identification of species that contribute to film growth and for elucidation of plasma mechanisms.

There are few studies that have directly investigated the surface interactions of CF_x radicals during polymer deposition. Some studies have, however, correlated gas-phase species density with film growth rates. Kitamura and coworkers used laser-induced fluorescence (LIF) to detect CF_2 in C_2F_6 plasmas.[13] They observed a third order dependence of the CF_2 normalized LIF intensity to the polymer deposition rate with increasing applied rf power. Spatially resolved LIF measurements of CF_2 intensity radially across the deposition electrode also showed a strong correlation with CF_2 intensity and polymer film thickness. Under low growth rate conditions (100% CF_4 plasmas), Booth and coworkers have measured steady-state concentration profiles for CF and CF_2 radicals using different substrate materials.[14,15] Their spatially-resolved radial measurements suggest there is small production of CF_2 radicals on Al and SiO_2 substrates, and much higher surface production on Si substrates. They also find that energetic ion bombardment is a necessary component of the observed radical production.[15,16]

Our imaging of radicals interacting with surfaces (IRIS) technique directly measures the steady-state surface reactivity of a gas-phase species during plasma processing. IRIS combines molecular beam and plasma technologies with laser-

induced fluorescence (LIF) to provide spatially resolved 2D images of radical species involved in film formation or etching.[17] To date, the IRIS method has been used to investigate seven different radical species[18,19,20] in several different plasma systems.[21,22] Most recently, we have focused on the surface reactivity of CF_x radicals in FCPs.[23,24,25] Here, in addition to surface reactivity data for CF_2 radicals in CHF_3 and 50/50 C_2F_6/H_2 plasmas, we present optical emission spectroscopy (OES) of the FCPs. Moreover, we correlate these gas-phase measurements with X-ray photoelectron spectroscopy (XPS) and Fourier transform infrared (FTIR) spectroscopy analyses of fluorocarbon films deposited during IRIS experiments. Thus, this fairly complete description of the plasma systems allows us the opportunity to offer insight into the plasma deposition mechanism.

Experimental Methods

The IRIS method has been described in detail previously.[17] In a typical IRIS experiment, feed gases enter the glass tube source region, rf power is applied, and a plasma is produced. Expansion of the plasma into a differentially pumped vacuum chamber, and ultimately into a high vacuum region, generates an effusive molecular beam consisting of virtually all species present in the plasma, including the species of interest. A tunable laser beam intersects the molecular beam downstream from the plasma source at a 45° angle and excites the radical of choice. Spatially resolved LIF signals are collected by an electronically gated, intensified charge coupled device (ICCD) located perpendicular to both the molecular beam and the laser beam, directly above the interaction region. A substrate is rotated into the path of the molecular beam and LIF signals are again collected. Differences between the spatial distributions with the surface in and out of the molecular beam are used to measure a radical's surface reactivity.

We can interpret the spatially-resolved LIF data with our quantitative model of the experiment,[18] which reproduces the scattering data in one dimension.[19] Briefly, the simulation is based on the known geometry of the experiment and calculates the spatial distribution of the radical number density in the molecular beam at the interaction region. Our model also calculates the radical number density along the laser beam for molecules scattering from the substrate surface assuming adsorption-desorption scattering. The calculated curve for this type of scatter assumes all of the incident radicals leave the substrate surface with a cosine distribution about the surface normal. To determine the surface reactivity of a specific molecule, the fraction of radicals scattering from the surface, S, is adjusted to best fit the experimental data. We define surface reactivity, R, as $1\text{-}S$. R can be considered as an effective surface reaction probability for a given species.[26] Here, we will discuss the surface interactions of CF_2 primarily from the standpoint of scatter, S.

The source of the molecular beam is a continuous wave (CW) plasma consisting of 100% CHF_3 (Air Products, 99.95%), or a 50/50 mixture of C_2F_6 (Air Products 99.995%) and H_2 (General Air 99.99%). Total pressure in the source is 60-80 mTorr CHF_3 and 25-30 mTorr for C_2F_6/H_2 as measured by a capacitance

manometer. The plasma is produced by the inductive coupling of 13.56 MHz rf power (50 or 100 W) tuned by an rf matching network. The molecular beam was collimated by two rectangular slits, 1.03 and 1.25 mm wide, mounted on a liquid nitrogen cold shield maintained at -200°C.[20]

Tunable laser light was produced by frequency doubling the output of an excimer-pumped (XeCl, 100 mJ, 100 Hz) dye laser system with Coumarin 47 (CF_2, 229-240 nm, 1.3 mJ/pulse). Substrates are p-type silicon (100) wafers with ~50 Å of native oxide placed 2.0 - 4.0 mm from the laser beam. For all CF_2 reactivity experiments shown here, the laser was tuned to 234.323 nm, corresponding to the (0,11,0) - (0,0,0) vibronic band of the A^1B_1 - X^1A_1 transition. LIF from the A^1B_1 (0,11,0) state of CF_2 was collected and focused directly onto the ICCD camera by two fused silica lenses as described previously.[23,24] All IRIS measurements are made in the saturated regime of laser power such that no corrections for fluctuations in laser power were made. Since the IRIS method is based on normalizing the signal from scattered radicals to the signal from radicals in the incident molecular beam, our measurements are not adversely affected by small fluctuations in laser power.

LIF signals were collected for 5 accumulations of 10-30 s exposure each for CF_2 and multiple sets of data were taken for each experiment. Background images were taken with the laser tuned to an off-resonance frequency and were subtracted from the data image. A 1-D representation of the image was made by averaging 20 columns of pixels (7.74 mm) containing the LIF signal and plotting signal intensity as a function of distance along the laser beam path. The ICCD camera had a 0.3 μs gate width for CF_2 molecule (radiative lifetime 61 ± 3 ns[27]).

Reflection IR spectra of deposited films were obtained with a Nicolet Magna 760 FTIR at 2 cm^{-1} resolution. XPS analyses were performed on a Surface Science Instruments S-probe spectrometer at the NESAC/BIO center at the University of Washington, which has a monochromatic Al Kα X-ray source ($h\nu$ = 1486.6 eV), hemispherical analyzer, and resistive strip multichannel detector. Details of the apparatus configuration and correction of the binding energy (BE) scales for these measurements are given elsewhere.[24]

Optical emission spectra (OES) from 240 - 713 nm were obtained for the FCPs using an inductively coupled plasma reactor nearly identical to the one used as the molecular beam source in IRIS experiments.[28] Emitted light was collected through a quartz window situated 10 mm downstream of the coil region, resulting in coaxial sampling of the plasma emission. Emission was imaged onto the 10 μm entrance slit of an Ocean Optics S2000 spectrograph using an optical fiber. The spectrograph was equipped with a 1800 grooves/mm holographic grating and a 2048-element linear CCD-array detector. Deposition rates were measured using a Tencor alpha step 100 profilometer. Details on deposition rates for the C_2F_6/H_2 system are provided in Ref. 28.

Results

LIF Excitation Spectra of CF_2. LIF measurements of CF_2 radicals were made in the IRIS apparatus with no substrate in the path of the molecular beam.

LIF provides a direct spectroscopic tool for identification and independent study of a specific ground-state radical in a molecular beam populated with many species. Figure 1 shows excitation spectra of CF_2 from 50/50 C_2F_6/H_2 and 100% CHF_3 plasmas (50 W) taken by stepping the laser from 227 to 240 nm in 0.025 nm increments (1s/step). Comparison to literature spectra verifies that the fluorescing species is indeed CF_2,[27] and demonstrates there are no contributions from any other molecular beam species in this wavelength range. Therefore, we are assured that the LIF signals we collect for subsequent experiments are solely LIF from CF_2 radicals.

Optical Emission Spectroscopy. OES is also a useful spectroscopic tool that allows for the identification of excited state species in a plasma. Here, we collect emission spectra for our two plasma systems using the independent plasma reactors described previously.[28] Plasma emission in the range 240 to 713 nm was analyzed from 100% CHF_3 and 50/50 C_2F_6/H_2 plasmas (50 W), Figure 2. The spectrum of the 50/50 C_2F_6/H_2 plasma is dominated by CF_2 emission from the bending mode of the A^1B_1 - X^1A_1 system, characterized by vibronic transitions $A(0,\nu_2, 0)$ - $X(\nu_1, \nu_2, 0)$ from 249 to 300 nm, Figure 2a.[5] The small peak at 387 nm is assigned to N_2 emission, which is a residual component of our plasma reactor. In addition, there are peaks attributed to H_α and H_β atomic emission at 656.3 nm and 486.1 nm respectively.[29] The 100% CHF_3 emission spectrum is similar, exhibiting a strong CF_2 emission, Figure 2b. One major difference, however, is that the H_α emission is significantly less intense than observed for the 50/50 C_2F_6/H_2 plasma

Surface Reactivity of CF_2. Figure 3 shows a series of ICCD images of CF_2 using a 100% CHF_3 plasma molecular beam and a Si substrate. The LIF signal from CF_2 molecules in the molecular beam is shown in Figure 3a. Figure 3b is the LIF signal acquired with a Si substrate rotated into the path of the molecular beam. Here, both the incident molecular beam and scattered CF_2 molecules are imaged. Figure 3c is the difference between Figures 3b and 3a and shows only CF_2 molecules scattered off the surface of the substrate.

Figure 4 shows the data of Figures 3a and 3c converted to a 1-D graphical representation for radicals both in the incident molecular beam and scattered, or desorbed, CF_2 molecules. The broad spatial distribution and the shift of the scattered signal peak maximum away from the molecular beam peak maximum indicate the CF_2 radicals scatter with a cosine angular distribution. Also shown in Figure 4 are simulated curves (dashed lines) for the incident beam and for scattered molecules assuming an adsorption-desorption mechanism, with $S = 1.65 \pm 0.05$. A scattering value greater than unity indicates that surface production of CF_2 (g) contributes to the observed scattering signal. Scattering values for CF_2 on other substrates, SiO_2, Si_3N_4, photoresist, and 304 stainless steel, are similar to that determined for silicon.[24]

Figure 5 shows cross sectional LIF data for CF_2 using a 50:50 C_2F_6/H_2 plasma molecular beam processing a silcon substrate. Here, the relative intensity of the scattered signal has decreased significantly from the 100% CHF_3 data. Simulating the 50:50 C_2F_6/H_2 experiment as above yields $S = 0.86 \pm 0.09$. This is a considerably lower scatter than was observed above with a 100% CHF_3 plasma

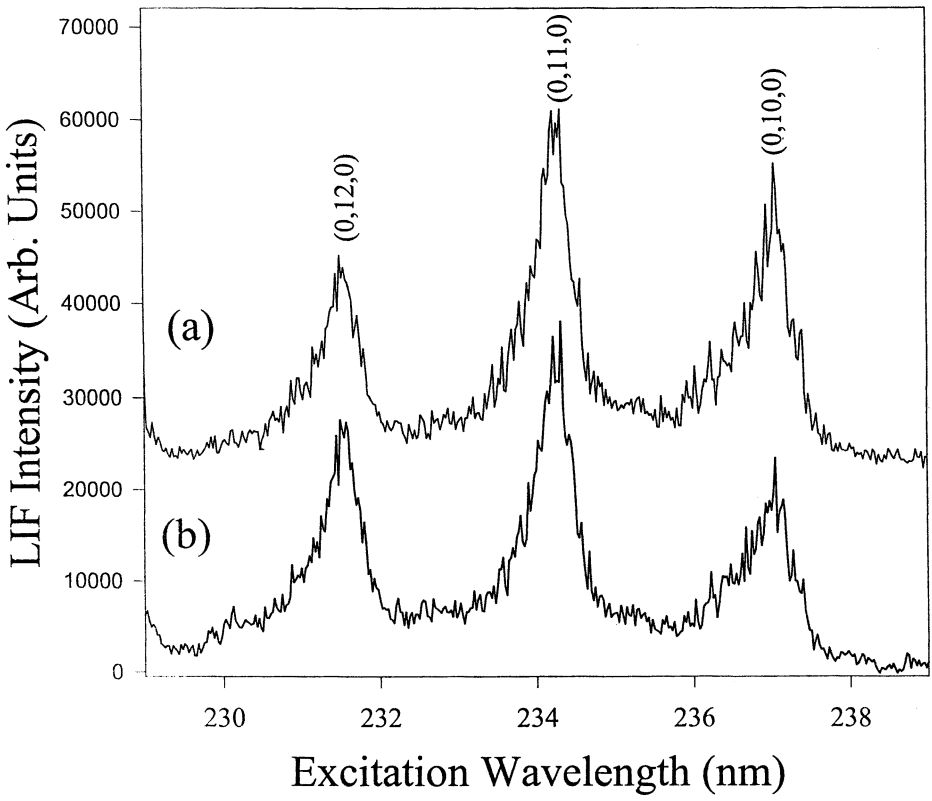

Figure 1. Experimental fluorescence excitation spectra of CF_2 in (a) 50/50 C_2F_6/H_2 and (b)100% CHF_3 plasma molecular beam from 227 to 239 nm. The transition used for all reactivity experiments was the (0,11,0) vibronic band of the A^1B_1 - X^1A_1 transition.

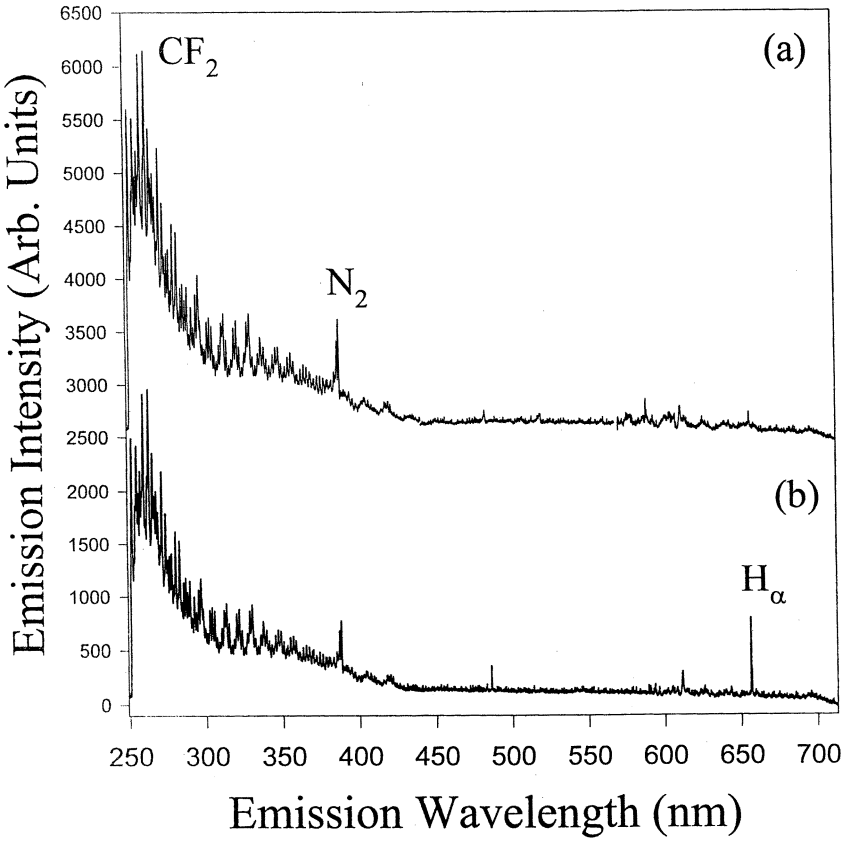

Figure 2. Optical emission spectra of (a) 50/50 C_2F_6/H_2 and (b)100% CHF_3 plasma from 249 to 713 nm. Spectra collected coaxially from an independent inductively coupled rf plasma reactor.

Publication Date: February 15, 2001 | doi: 10.1021/bk-2001-0787.ch013

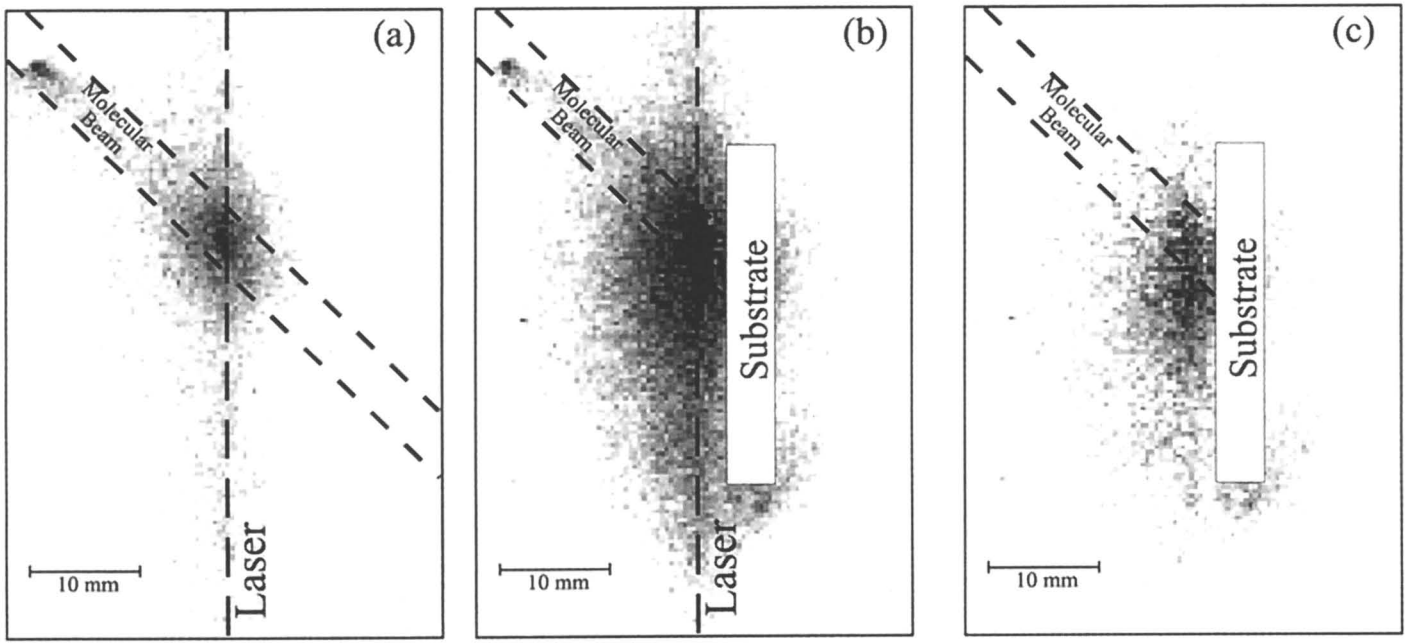

Figure 3. Spatially resolved two-dimensional ICCD images of the LIF signal for the CF_2 (0,11,0) state (a) in the 100% CHF_3 molecular beam (no substrate) and (b) with a 300 K Si substrate rotated into the path of the molecular beam at a laser-surface distance of 3 mm. (c) Difference between the images shown in (a) and (b), corresponding to CF_2 molecules scattering from the surface. LIF signals with the highest intensity appear as the darkest regions in the images. Dashed lines indicate the location of the molecular beam and the laser beam.

In Fluorinated Surfaces, Coatings, and Films; Castner, David G., et al.;
ACS Symposium Series; American Chemical Society: Washington, DC, 2001.

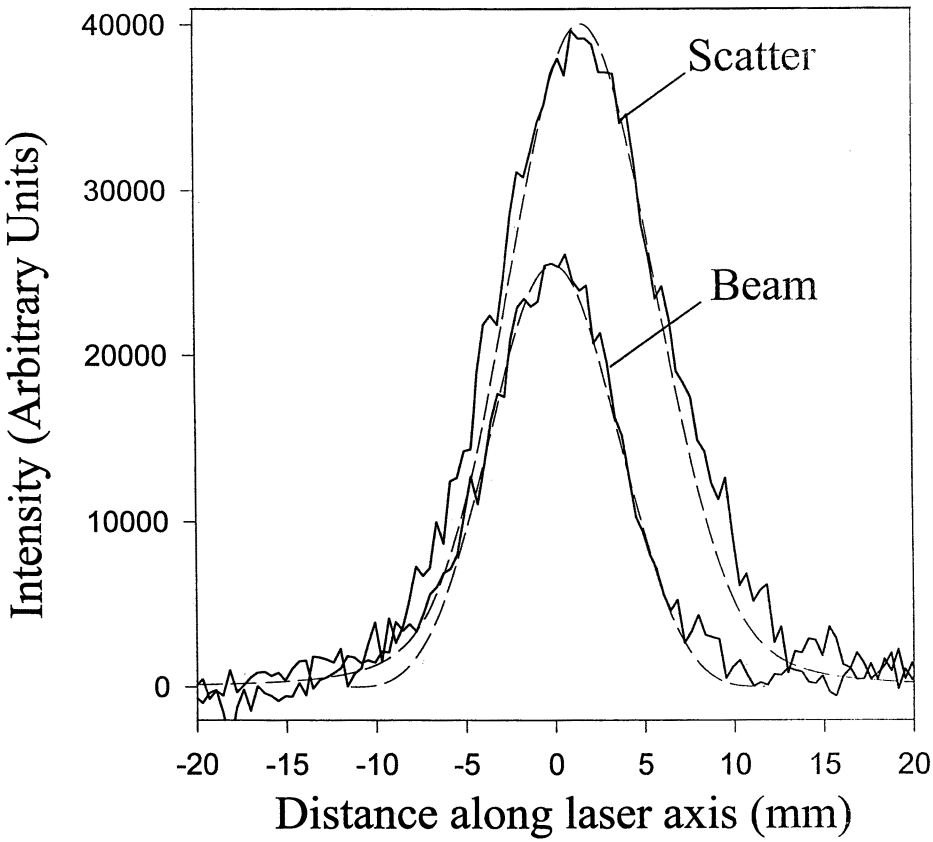

Figure 4. Cross-sectional data for the LIF of CF_2 in the incident molecular beam and scattered from the Si (100) substrate using a 100% CHF_3 plasma molecular beam. The laser-surface distance is 3.0 mm. Dashed lines represent the simulated curves from the geometric model, assuming $S = 1.65$ and adsorption-desorption scattering.

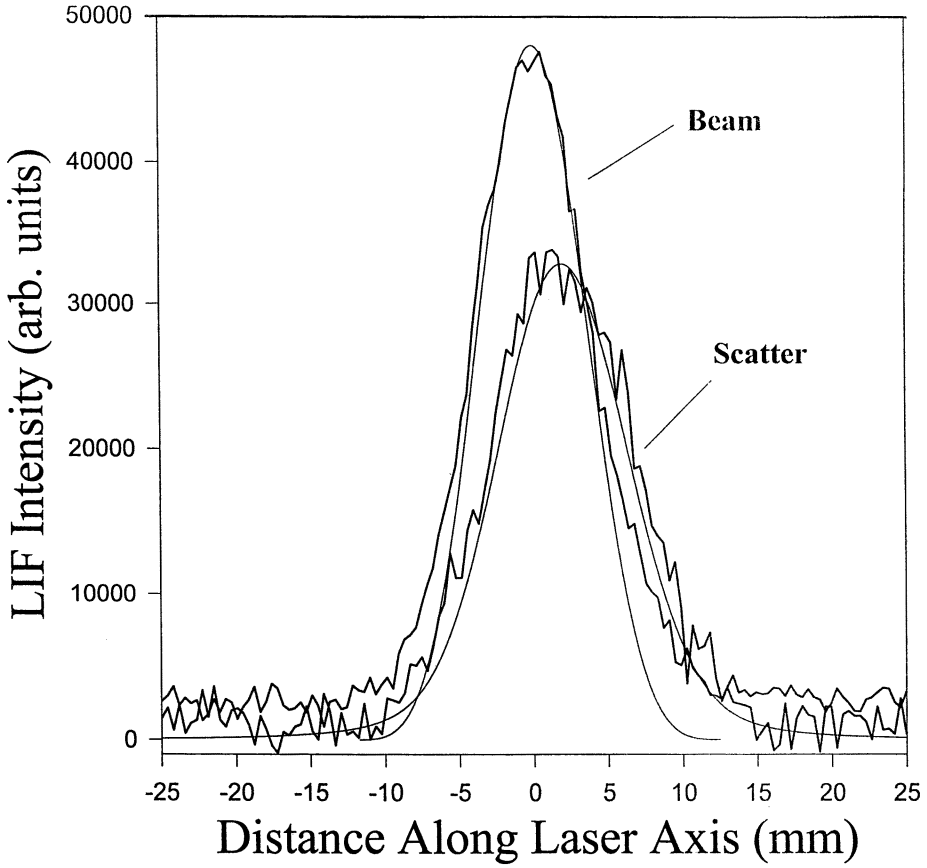

Figure 5. Cross-sectional data for the LIF of CF_2 in the incident molecular beam and scattered from the Si (100) substrate using a 50/50 C_2F_6/H_2 plasma molecular beam. The laser-surface distance is 3.0 mm. Dashed lines represent the simulated curves from the geometric model, assuming $S = 0.84$ and adsorption-desorption scattering.

molecular beam and this polymeric substrate. This result indicates that in this FCP system, CF_2 is removed from the gas phase during plasma polymerization. Values for CF_2 scatter from SiO_2, and polyimide surfaces using a 50/50 C_2F_6/H_2 plasma were similar to the value determined for Si.[25]

Deposition rates of fluorocarbon films. Due to low molecular beam species flux and corresponding low deposition rates in our IRIS experiment, deposition rates were determined for films deposited from 50/50 C_2F_6/H_2 and 100% CHF_3 in an inductively coupled plasma reactor nearly identical to the source on IRIS.[28] In general, deposition rates for C_2F_6/H_2 are five times faster than for films deposited from CHF_3 under identical conditions, Fig. 6. Deposition rates from C_2F_6/H_2 plasmas increase rapidly from 10 to 30 W to a value of 770 Å/min. The deposition rate goes through a maximum at 100 W where it reaches 1200 Å/min and decreases at higher powers to ~800 Å/min. In contrast, the deposition rate from CHF_3 plasmas increases initially, then remains constant at a rate of 100 Å/min from 25-150 W applied power. The deposition rate then increases to a value of 400 Å/min at the highest applied power used, 200 W.

Characterization of fluorocarbon films. To correlate our radical surface reactivities with the composition of the deposited material, IRIS substrates were removed from the instrument after reactivity measurements were completed and surface analysis was performed. Figure 7 shows C_{1s} spectra for films deposited on silicon substrates during IRIS experiments using 50/50 C_2F_6/H_2 and CHF_3 plasmas. Analysis shows the experimental curves can be fit using a series of peaks assigned to CF_3, (BE = 294 eV), CF_2 (BE = 292.1 eV), CF (BE = 289.5 eV), C- CF (BE = 287.3), and CH (285 eV).[5] Elemental composition and C1s contributions for these films are listed in Table I.

Table I. XPS C1s and elemental composition for films deposited on Silicon from 100% CHF_3 and 50/50 C_2F_6/H_2 plasmas

	C1s Contribution %						Elemental Composition %				
Plasma	CH	C-CF	CF	CF_2	CF_3	F/C	F	C	O	N	Si
100% CHF_3	17	29	27	20	7	0.8	41.4	50.7	5.4	2.6	-
50/50 C_2F_6/H_2	13	29	27	19	12	1.0	48.2	48.4	3.1	-	0.3

Figure 8 shows FTIR spectra of amorphous fluorocarbon polymers deposited on Si substrates from 100% CHF_3 and 50/50 C_2F_6/H_2 plasmas. Films deposited from 50/50 C_2F_6/H_2 plasmas during IRIS experiments were analyzed directly. To obtain an acceptable FTIR absorbance, films were deposited from 100% CHF_3 in an

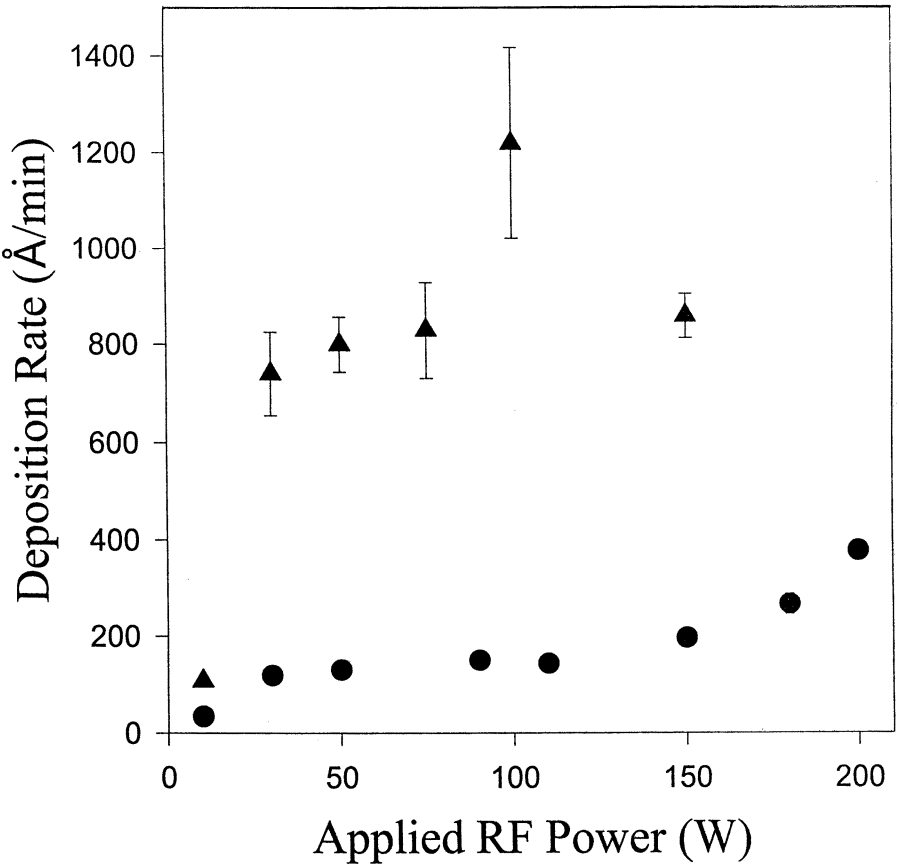

Figure 6. Deposition rates for films deposited for 10-15 minutes from 50/50 C_2F_6/H_2 (closed triangles) and 100% CHF_3 (closed circles) plasmas. All films were deposited in an independent inductively coupled rf plasma reactor.

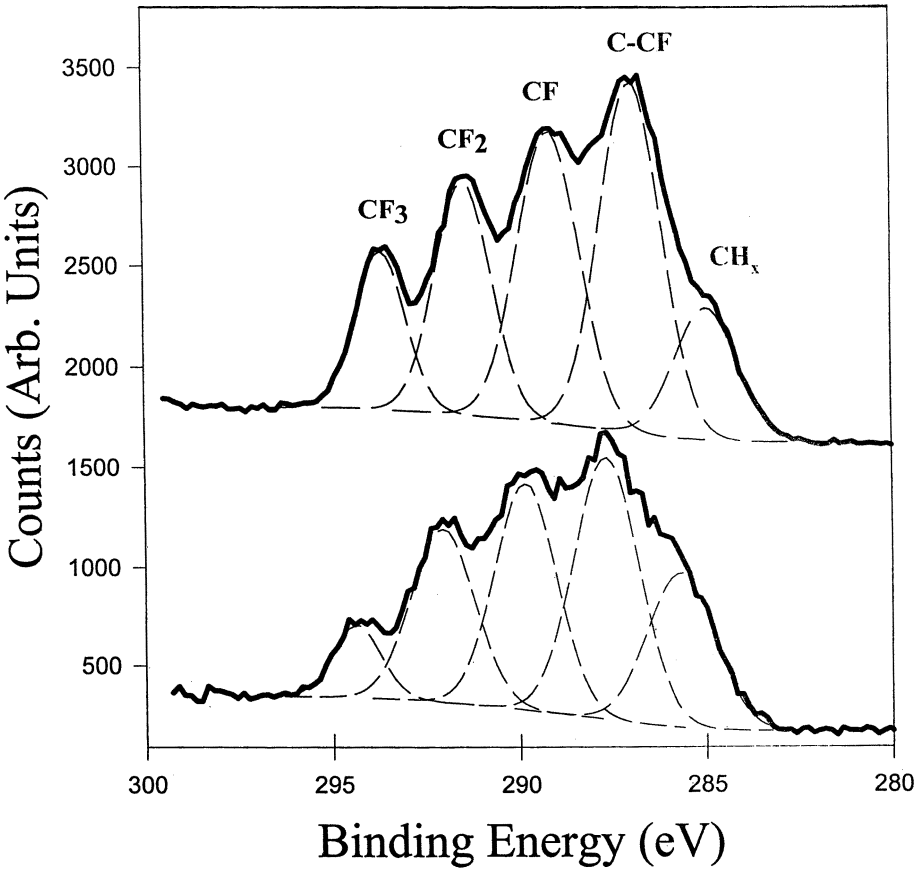

Figure 7. XPS C_{1s} spectra of fluorocarbon films deposited during IRIS experiment using (a) 50/50 C_2F_6/H_2 and (b) 100% CHF_3 plasma molecular beam. Spectra were taken at a photoelectron take-off angle of 55° from the surface normal.

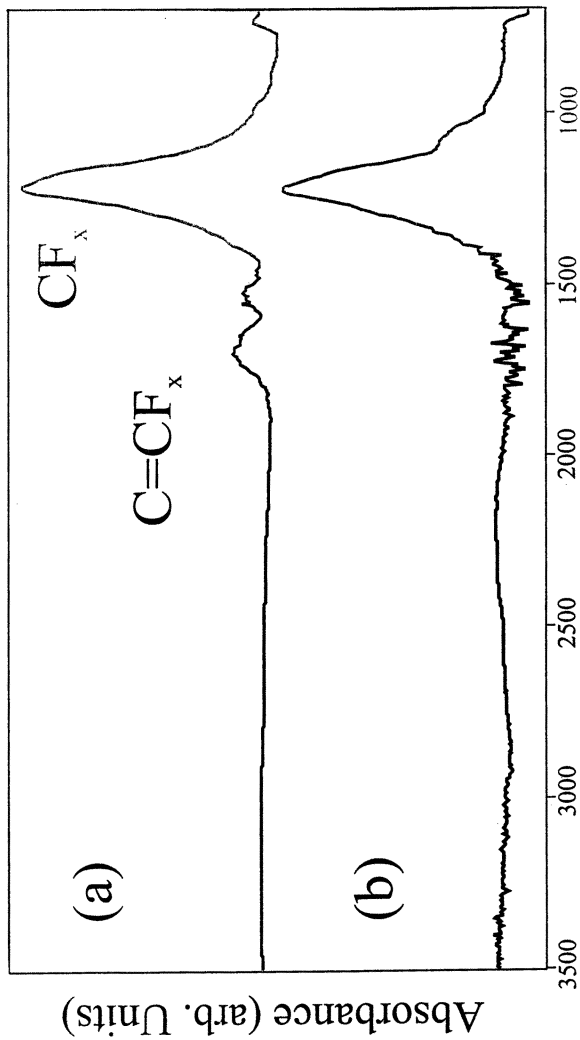

Figure 8. FTIR transmission spectra of fluorocarbon films deposited from a (a)100% CHF_3 50/50 plasma from an independent inductively coupled rf plasma reactor, and (b) C_2F_6/H_2 plasma during an IRIS experiment.

independent inductively coupled plasma reactor described in the previous section. Conditions for these depositions were 50 W applied rf power and 100mTorr pressure in the reactor. The film deposited from 100% CHF_3 shows two major absorption bands, one at 1100 - 1400 cm^{-1} and another, smaller peak at ~1700 cm^{-1}, Fig. 8a. These peaks are attributed to CF_x (x = 1-3) and unsaturated stretching modes, respectively.[30] Aydil and coworkers have observed this type of unsaturation in films deposited from CF_4/H_2 plasmas under deposition conditions, i.e. >25% H_2. Under etching conditions, the degree of unsaturation decreases significantly.[31] Further analysis of the spectra reveal a A(C=C)/A(C-F) ratio of 0.20 ± 0.01 for the 50 W data. This is consistent with the results of Aydil and coworkers for conditions where the fluorocarbon layer thickness increases with time. Amorphous fluorocarbon films are also deposited from 50/50 C_2F_6/H_2 and are similar to films deposited from CHF_3 plasmas in that they contain an amorphous CF_x band at 1100 - 1400 cm^{-1}, however, the degree of unsaturation in these fluorocarbon polymer films is much lower.

Discussion

Although FCPs have been studied extensively, past studies have rarely discussed both gas-phase characterization and substrate processing effects. Indeed, most researchers concentrate on only one aspect of these complicated systems. Yet, determining how gas-phase radicals interact with a substrate is critical to understanding the chemistry of plasma processing. This is especially important in FCPs as the balance between film growth and etching depends on the interactions of active plasma species with the substrate being processed. Insight into the reactions of radicals with a surface *during* plasma processing under different plasma conditions can be obtained with IRIS measurements. IRIS allows the study of one specific molecule interacting with a specific surface while it is being bombarded by the full range of plasma species.

Comparison of the two fluorocarbon systems studied here illuminates the similarities and differences in the chemical and physical process that occur during plasma polymerization of fluorocarbon materials. First, amorphous fluorocarbon polymer films are deposited from both 100% CHF_3 and 50/50 C_2F_6/H_2 plasmas. Our XPS and FTIR analyses reveal the chemical composition of these materials are very similar and indicate a high degree of crosslinking which is likely the result of ion bombardment.[28,32] Deposition rates in the two systems, however, are significantly different. Indeed, the deposition rate for the 50/50 C_2F_6/H_2 system is at least a factor of four higher than in the CHF_3 system. Second, from our OES data, we find that both precursors decompose to generate CF_2 and H atoms, although in very different amounts, with the higher CF_2 radical and H atom content occurring in the C_2F_6/H_2 system.

Most significantly, the surface interactions of CF_2 radicals during polymer deposition measured with IRIS are very different in the two systems. Our IRIS data clearly indicate we have consumption of CF_2 ($S = 0.86 \pm 0.09$) on Si substrates using 50/50 C_2F_6/H_2 plasmas. Consumption of radicals in IRIS experiments during plasma deposition is generally thought to indicate the radical species is contributing

to film growth.[17] In contrast, we have a high degree of scatter for CF_2 radicals (S = 1.65 ± 0.05) on Si substrates using 100% CHF_3 plasmas. This demonstrates that CF_2 is generated at the surface during film deposition in this system. We have previously discussed several possible surface reactions that could account for the observed production of CF_2 radicals in FCPs.[23,24] Briefly, these include dissociative adsorption of molecular beam species, such as CF_3 (producing CF_2 and an adsorbed F atom); surface F atom abstraction by CF radicals; and ion assisted sputtering of the deposited fluorocarbon polymer. Based on results from experiments employing a grounded mesh screen to remove ions from our molecular beam, we believe ion bombardment is a significant source of CF_2 in the CHF_3 system.[24]

The observations that high CF_x content and ion bombardment affect CF_2 surface reactivities are consistent with d'Agostino and coworkers' proposed activated growth model (AGM) for the formation of polymeric films in FCPs.[5] One of the key points of the AGM is that a relatively high density of fast electrons or energetic ions is necessary for the growth process. These high energy species are responsible for the formation of activated polymer sites on the growing film surface. Indeed, d'Agostino and coworkers found that deposition kinetics depend on both CF_x (x = 1, 2) concentration and on the flux and/or energy of positive ions.[5] Moreover, they observed that when the energy of ions is roughly equivalent to that of a floating or a biased substrate (i.e. with voltages < 50-70 eV), deposition rates increased with both fluxes of radicals and ions (or simply with ion energy).[33] With more energetic ions, however, ion-assisted etching starts to compete with deposition; thus, the deposition rate goes through a maximum when plotted against the bias voltage.[34]

As noted above, the H atom content is significantly greater in the C_2F_6/H_2 plasma, even though the C/F/H mole ratios (1:3:1) in the two FCP systems are identical. It is well known that the deposition rate for fluorocarbon polymers from saturated perfluorinated precursors is directly related to the amount of H_2 added to the system, with a maximum at ~50% H_2 addition. Moreover, Aydil and coworkers have shown that fluorocarbon polymers exposed to a H_2 plasma are surface modified via replacement of F atoms in the polymer by H atoms.[32] This replacement occurs through abstraction of surface fluorine by hydrogen and subsequent reaction between gas-phase H atoms and the newly created active surface site. In the C_2F_6/H_2 system, not only do we have H atom flux to the surface, we also have CF_x flux to the surface. Thus, it is conceivable that the active surface sites created by F abstraction react with both H atoms and CF_x radicals, resulting in a relatively rapid deposition rate. In the CHF_3 system, the H atom flux to the surface is lower, as is the CF_x flux, therefore we observe a much slower deposition rate.

FCPs are unique in that the relative importance of active species (CF_x radicals and energetic charged particles) can be continuously varied by controlling the plasma parameters and feed gas content. This means that the etching or polymerizing capacity of FCPs can be tailored to suit a particular application. This is exemplified by the two systems we study here. In the 50/50 C_2F_6/H_2 system, the deposition rate is at a maximum,[28] implying the active species contribute primarily

to deposition and etching is minimized. This suggests that ion bombardment of the surface is only serving to create active sites for film growth, and is not ablating a significant amount of the deposited material. Consequently, in our IRIS experiments, we observe net consumption of CF_2, rather than generation. In the CHF_3 system, the active species are also contributing to deposition, but at a much slower rate. This suggests that both etching and deposition are occurring at nearly equal rates. Thus, ion bombardment of the surface serves primarily to ablate the depositing fluorocarbon material rather than to create active sites. This is also supported by our IRIS results for CF_2 in a primarily etching system, 100% C_2F_6 plasmas. In this system, CF_2 was generated at the surface of a Si substrate ($S = 1.44 \pm 0.03$) and no net deposition was measured.

Conclusions

Fluorocarbon deposition mechanisms have been investigated using our unique IRIS technique in combination with extensive surface analysis of deposited films and optical emission spectroscopy of the C_2F_6/H_2 and CHF_3 plasmas. IRIS measurements for CF_2 radicals in the two plasma systems demonstrate two very different types of surface interactions. In the C_2F_6/H_2 plasma, CF_2 radicals are consumed during rapid deposition of a thick fluorocarbon polymer film. In contrast, in the CHF_3 system, CF_2 radicals are generated at the surface during much slower film deposition. These differences in surface reactivity and deposition rates are explained by consideration of the relative fluxes of active species in both systems and by the role of H atoms in the passivation of the fluorocarbon film. Additional clarification of the role of charged species as well as IRIS measurements for other CF_x radicals are clearly needed to further understand the chemistry of FCPs.

Acknowledgments

We thank Prof. David G. Castner of the University of Washington for performing XPS analyses on our fluorocarbon films. This work is supported by the National Science Foundation (CHE-951157).

References

1. Miyata, K.; Hori. M.; Goto, T. *J. Vac. Sci. Technol. A* **1997,** *15*, 568.

2. Inayoshim M.; Iti, M.; Hori, M.; Goto, T.; Hiramatsu, M. *J. Vac. Sci. Technol. A* **1998,** *16*, 233.

3. Kadono, M.; Inoue, T.; Miyanaga, A.; Yamazake, S. *Appl. Phys. Lett.* **1992,** *61*, 772.

4. d'Agostino, R.; Lamendola, R.; Favia, P.; Giques, A. *J. Vac. Sci. Technol. A* **1994,** *12*, 308; Sah, R.; Dishler, E. B.; Bubenzer, A.; Koidl, P. *Appl. Phys. Lett.* **1985,** *46*, 739.

5. d'Agostino, R.; Cramarossa, F.; Fracassi, F.; Illuzzi F. in *Plasma Deposition, Treatment and Etching of Polymers*, R. d'Agostino, Ed., Academic Press: San Diego, CA, **1990,** pp. 95.

6. Suzuki, C.; Kadota, K. *Appl. Phyd. Lett.* **1995**, *67*, 2569.

7. O'Neil, J. A.; Singh, J. *J. Appl. Phys.* **1994**, *76*, 5967.

8. Takahashi, K.; Hori, M.; Goto, T. *J. Vac. Sci. Technol. A* **1996**, *14*, 2004.

9. d'Agostino, R.; Cramarossa, F.; Illuzzi, F. *J. Appl. Phys.* **1987**, *61*, 2754.

10. d'Agostino, R.; Cramarossa, F.; Fracassi, F.; DeSimoni, E.; Sabbarini, L.; Zambonin, P. G.; Caporicco, G. *Thin Solid Films* **1986**, *143*, 163.

11. Hikosaka, Y.; Toyoda, H.; Sugai, H. *Jpn. J. Appl. Phys.* **1993**, *32*, L690; O'Keefe, M. J.; Rigsbee, J. M.; *J. Appl. Polym. Sci.* **1994**, *53*, 1631.

12. Takahashi, K.; Hori, M.; Maruyama, K.; Kishimoto, S.; Goto, T. *Jpn. J. Appl. Phys.* **1993**, *32*, L694.

13. Kitamura, M. Akiya, H, Urisu, T. *J. Vac. Sci. Technol. B.* **1989**, *7*, 14.

14. Booth, J. P.; Cunge, G.; Chabert, P.; Schwarzenbach, W. In *Frontiers in Low Temperature Plasma Diagnostics II*, Bad Honnef, Germany, **1997**, 147.

15. Tserepi, A. D.; Derouard, J.; Booth, J. P.; Sadeghi, N. *J. Appl. Phys.* **1997**, *81*, 2124.

16. Cunge, G. Ph.D. Thesis, **1997**, Laboratoire de Spectrometrie Physique, Université Joseph Fourier, BP 87, 38402 St Martin d'Hères Cedex; J. P. Booth, private communication.

17. McCurdy, P. R.; Bogart, K. H. A.; Dalleska, N. F.; Fisher, E. R. *Rev. Sci. Instrum.* **1997**, *68*, 1684.

18. Bogart, K. H. A.; Cushing, J. P.; Fisher, E. R. *Chem. Phys. Lett.* **1997**, 267, 377.

19. Bogart, K. H. A.; Cushing, J. P.; Fisher, E. R. *J. Phys. Chem.* **1997**, *101*, 10016.

20. McCurdy, P. R.; Venturo, V. A.; Fisher, E. R. *Chem. Phys. Lett.* **1997**, *274*, 120.

21. Buss, R. J.; Ho, P. *IEEE Trans. Plasma Sci.* **1996**, *24*, 79.

22. Buss, R. J.; Ho, P.; Weber, M. E. *Plasma Chem. Plasma Process.* **1993**, *13*, 61.

23. Mackie, N. M.; Venturo, V. A. Fisher, E. R. *J. Phys Chem* **1998**, *101*, 9425.

24. Capps, N. E.; Mackie, N. M. Fisher, E. R. *J. Appl. Phys.* **1998**, *84*, 4736.

25. Butoi, C. I., Mackie, N. M.; Williams, K. L.; Capps, N. E.; Fisher, E. R. *J. Vac. Sci. Technol. A,* submitted for publication.

26. Perrin, J.; Shiratani, M.; Kae-Nune, P.; Videlot, H.; Jolly, J.; Guillon, J. *J. Vac. Sci. Technol. A* **1998**, *16*, 278.

27. King, D. S.; Schenck, P. K.; Stephenson, J. C. *J. Mol. Spectrosc.* **1979**, *78*, 1.

28. Mackie, N. M.; Dalleska, N. F.; Castner, D. G.; Fisher, E. R. *Chem. Mater.* **1997**, *9*, 349.

29. Barshilia, H. C.; Mehta, B. R.; Vankar, V. D. *J. Mater. Res.* **1996**, *11*, 2852.

30. Colthup, N. B.; Daly, L. H.; Wiberley, S. E. *Introduction to Infrared and Raman Spectroscopy*, 3rd Ed.; Academic Press: New York, 1990.

31. Marra D. C.; Aydil, E. S. *J. Vac. Sci. Technol. A* **1997**, *15*, 2508.

32. Yasuda, H. *Plasma Polymerization*; Academic Press: Orlando, FL, 1985.

33. d'Agostino, R., personal communication (1998).